

S100A8/A9 at low concentration promotes tumor cell growth via RAGE ligation and MAP kinase-dependent pathway

Saeid Ghavami,^{*,1} Iran Rashedi,^{*,1} Brian M. Dattilo,[†] Mehdi Eshraghi,^{*} Walter J. Chazin,[†] Mohammad Hashemi,[‡] Sebastian Wesselborg,[§] Claus Kerkhoff,^{11,2} and Marek Los^{11,2,3}

^{*}Manitoba Institute of Cell Biology and Department of Biochemistry and Medical Genetics, University of Manitoba, Winnipeg, Manitoba, Canada; ¹¹Institute of Experimental Dermatology, Münster, Germany; [†]Departments of Biochemistry, Physics and Chemistry, Center for Structural Biology, Vanderbilt University, Nashville, Tennessee, USA; [‡]Department of Clinical Biochemistry, School of Medicine, Zahedan University of Medical Science, Zahedan, Iran; [§]Department of Internal Medicine I, University of Tübingen, Tübingen, Germany; and ¹BioApplications Enterprises, Winnipeg, Manitoba, Canada

Abstract: The complex formed by two members of the S100 calcium-binding protein family, S100A8/A9, exerts apoptosis-inducing activity against various cells, especially tumor cells. Here, we present evidence that S100A8/A9 also has cell growth-promoting activity at low concentrations. Receptor of advanced glycation end product (RAGE) gene silencing and cotreatment with a RAGE-specific blocking antibody revealed that this activity was mediated via RAGE ligation. To investigate the signaling pathways, MAPK phosphorylation and NF- κ B activation were characterized in S100A8/A9-treated cells. S100A8/A9 caused a significant increase in p38 MAPK and p44/42 kinase phosphorylation, and the status of stress-activated protein kinase/JNK phosphorylation remained unchanged. Treatment of cells with S100A8/A9 also enhanced NF- κ B activation. RAGE small interfering RNA pretreatment abrogated the S100A8/A9-induced NF- κ B activation. Our data indicate that S100A8/A9-promoted cell growth occurs through RAGE signaling and activation of NF- κ B. *J. Leukoc. Biol.* 83: 1484–1492; 2008.

Key Words: NF- κ B · proliferation · MRP8 · MRP14 · endokines · S100/calgranulins · cytotoxic peptides

INTRODUCTION

The S100 protein family is a multigenic group of nonubiquitous, cytoplasmic EF-hand Ca²⁺-binding proteins, which are expressed in a wide variety of cell types [1]. In recent years, they have been linked to human pathologies as a result of their differential expression in chronic diseases and critical involvement in pivotal signal transduction pathways, including the receptor of advanced glycation end products (RAGE) [2]. An additional, important indication for their involvement in inflammatory and neoplastic disorders is that most S100 genes are found near a break-point region on human chromosome 1q21, which if affected, is responsible for a number of genetic abnormalities related to autoimmune pathologies or cancer [3,

4]. Although the function of S100 proteins in cancer cells in most cases is still unknown, the specific expression patterns of these proteins are a valuable prognostic tool [5].

Two S100 proteins, S100A8 and S100A9, have been linked to neoplastic disorders. Although they are predominantly expressed in myeloid cells, S100A8 and S100A9 are also found in the epidermis upon response to stress [6, 7] and in several tumor cell types. Immunohistochemical investigations have shown that these proteins are expressed in hepatocellular carcinomas, pulmonary adenocarcinoma, and invasive ductal carcinomas of the breast [8–10]. In these tumors, elevated expression is correlated with poor differentiation. S100A8 and S100A9 are also found to be enriched in cystic fluid and serum of patients with ovarian cancer [11]. Furthermore, their expression is enhanced in gastric cancer [12]. In contrast, S100A8 and S100A9 are frequently down-regulated in poorly differentiated, esophageal squamous cell carcinomas [13, 14].

Recently, we have reported a novel, proapoptotic effect of the S100A8/A9 protein complex formed by the two calcium-binding proteins S100A8 and S100A9 [15]. The S100A8/A9 protein complex is released from activated phagocytes and exerts apoptosis-inducing activity through a dual mechanism: one associated with zinc extraction from the target cells and the other through binding to the cell surface of the target cells, possibly via ligand-induced receptor activation. This finding is of great interest, as S100A8 and S100A9 are abundant in cells of the innate immune system, and S100A8/A9-positive cells accumulate along the invasive margin of cancer [16].

Several members of the S100 protein family have been reported to bind to RAGE [17–19], which is a multiligand receptor belonging to the Ig superfamily. It transduces inflammatory responses and the effects of neurotrophic and neurotoxic factors, plays a role in tumor growth [20, 21], and as shown recently, is involved in the pathogenesis of several

¹ These authors contributed equally to this work.

² These authors share senior authorship.

³ Correspondence: BioApplications Enterprises, 34 Vanier Dr., Winnipeg, R2V 2N6, MB, Canada. E-mail: mjelos@gmail.com

Received June 13, 2007; revised January 2, 2008; accepted January 16, 2008.

doi: 10.1189/jlb.0607397

diseases, including neurodegeneration, inflammation, and cancer [20, 21]. Although direct interaction of S100 proteins with RAGE has been shown only for S100A12 (ENRAGE), S100B, S100A1, and S100P [17, 19, 22], it has been suggested that RAGE may serve as a common extracellular S100 receptor, as the S100 proteins have common structural features and display sequence homology [17].

Huttunen et al. [18] communicated recently that nanomolar concentrations of S100B induce trophic effects in RAGE-expressing cells, whereas micromolar concentrations of S100B induce apoptosis in an oxidant-dependent manner. Therefore, we explored the effects of S100A8/A9 at low concentrations (<25 $\mu\text{g/ml}$) on tumor cells and signal transduction pathways. In this study, we showed that S100A8/A9 also displays a bimodal function, and its cell growth-promoting effect is mediated by RAGE-dependent signaling.

MATERIALS AND METHODS

Materials and reagents

Cell culture media were purchased from Sigma Co. (Oakville, ON, Canada) or Gibco (Canada). Cell culture plasticware was obtained from Nunc Co. (Canada); MTT and a BrdU incorporation ELISA kit were from Roche Applied Science (Canada); insulin-transferrin-selenium (ITS) supplements were from Invitrogen (Carlsbad, CA, USA); rabbit polyclonal anti-human, -murine, and -rat RAGE was from Abcam (Cambridge, MA, USA); U0126 and SB203580 were from Cell Signaling Technology (Beverly, MA, USA); FITC-labeled 27E10 mAb to human S100A8/A9 was from Acris (Germany); MAPK family antibody, sampler kit, and phospho-MAPK family antibody sampler kit were from Cell Signaling Technology; anti-human, -mouse, and -rat RAGE antibodies, human RAGE small interfering (si)RNA, and siRNA-negative control were from Santa Cruz Biotechnology (Santa Cruz, CA, USA); anti-human RAGE antibody and goat anti-human RAGE-blocking antibody were from R&D Systems (Hornby, ON, Canada); anti-human, -rat, and -murine high mobility group box 1 (HMGB1) was from Abcam; and a transbinding NF- κ B assay kit was from Panomics (Redwood City, CA, USA).

Purification of S100A8 and S100A9 from human neutrophils

Human neutrophils were prepared from leukocyte-rich blood fractions ("Buffy coat"). S100A8/A9 was purified as described earlier [23]. Prior to use, the proteins were rechromatographed by anion exchange using a UnoQ column (BioRad, Munich, Germany). Recombinant protein was produced by bacterial overexpression as described previously [24].

Cell culture

MCF-7 (human estrogen receptor-positive breast cancer), MDA-MB231 (human estrogen receptor-negative breast cancer), Jurkat (human T cell leukemia), BJAB (murine B cell leukemia), L929 (murine fibrosarcoma), human embryo kidney (HEK)-293, SHEP, and KELLY (human neuroblastoma) were cultured in RPMI 1640 or DMEM supplemented with 10% FCS, 100 U/ml penicillin, and 100 $\mu\text{g/ml}$ streptomycin. The cells were incubated at 37°C in a humidified atmosphere of 5% CO₂ and 95% air. Cells were maintained under logarithmic growth conditions.

Cell proliferation assay (MTT and BrdU assay)

Cells were starved in 1% ITS medium without FBS for 3 days. Then, various concentrations of S100A8/A9 were added for different time intervals as indicated, and cell viability was determined by the MTT assay as described previously [10, 11]. The percentage cell viability was calculated using the equation: (mean OD of treated cells/mean OD of control cells) \times 100. For confirmation, BrdU incorporation ELISA assay was performed according to the manufacturer's instruction.

Determination of S100A8/A9-binding sites on the cell surface

Harvested cells were washed three times with PBS containing 3% BSA and 0.05% sodium azide (B-PBS). A total of 2×10^6 cells was incubated with 10 μg human S100A8/A9 for 1 h, washed three times with B-PBS, and then incubated for 30 min in the dark with 200 μl FITC-labeled anti-S100A8/A9 antibody (1:50; murine IgG1 clone 27E10) containing 20 $\mu\text{g/ml}$ propidium iodide to gate out dead cells. Finally, they were washed three times with B-PBS. To determine nonspecific binding of the FITC-labeled anti-S100A8/A9, the cells were incubated with FITC-labeled antibody in the absence of human S100A8/A9. The stained cells were analyzed on a FACS machine at an excitation wavelength of 488 nm. Automated analyses were performed using CellQuest Pro software.

Protease protection assay

Limited proteolysis was performed at room temperature on proteins dialyzed against 10 mM HEPES-NaOH, 75 mM NaCl, at pH 7.0. The preparation of the tandem variable-constant 1 (VC1) fragment of RAGE has been described previously [19]. For each experiment, 50–100 μg purified protein was incubated with chymotrypsin at an enzyme:protein ratio of 1:500 (w/w) in a volume of 100 μl . The reaction was stopped at indicated time-points by aliquoting 14 μl reaction mix into 14 μl 2 \times SDS loading buffer and heating at 90°C for 5 min. For the VC1-S100A8/A9 complex, S100A8/A9 was mixed with VC1 at a 2:1 molar stoichiometry, and CaCl₂ was added to a final concentration of 1 mM prior to the addition of enzyme. Control experiments with S100A8/A9 alone and VC1 were performed under identical conditions (i.e., in the presence of Ca²⁺) [19].

Immunoblotting

RAGE expression was analyzed by Western blot. The same method [25] was used to detect p38 MAPK, p44/p42 MAPK, stress-activated protein kinase (SAPK)/JNK, phospho-p38 MAPK, phospho-p44/42 MAPK, and phospho-SAPK/JNK in MCF-7 and MDA-MB231 cells that had been treated with 10 $\mu\text{g/ml}$ S100A8/A9 for different time intervals. Cell lysates were prepared. Briefly, the harvested cells were washed once with cold PBS and resuspended for 20 min on ice in a lysis buffer: 20 mM Tris-HCl (pH 7.5), 0.5% Nonidet P-40, 0.5 mM PMSF, and 0.5% protease inhibitor cocktail (Sigma Co.). The high-speed supernatant (10,000 g) was collected. Proteins (30 μg) were separated by SDS-PAGE, then transferred onto nylon membranes, which were blocked in 5% nonfat dried milk in 1% TBS (0.05 M Trizma base, 0.9% NaCl, and 1% Tween-20), and then incubated overnight with the primary antibodies at 4°C. The membranes were then incubated at room temperature for 1 h with the relevant secondary antibodies conjugated with HRP and developed by ECL detection (Amersham-Pharmacia-Biotech, Piscataway, NJ, USA). In experiments detecting soluble (s)RAGE and HMGB1, cells were treated with S100A8/A9 (15 $\mu\text{g/ml}$) for different time intervals as indicated. In other experiments, cells were treated with different concentrations of S100A8/A9 (0, 10, 20, 25 $\mu\text{g/ml}$) for 36 h. The cell culture medium was collected and centrifuged at 10,000 g for 10 min to precipitate the floating cells and cells debris. Then, the supernatants were collected and centrifuged in 50 ml tubes, which were equipped with filters that kept the protein over 15 kDa. Finally, protein concentration was measured by Bradford, and equal amounts of protein were subjected to SDS-PAGE followed by Western blotting.

RNA interference

The target siRNA for RAGE (sc-36374) and a negative-control siRNA (sc-37007) with an irrelevant sequence were purchased from Santa Cruz Biotechnology. The cells were grown to 60–80% confluence and then transfected with the siRNA duplex (final concentration, 100 nM) using Lipofectamine (Invitrogen), according to the manufacturer's instructions. RAGE expression was determined by immunoblotting at 0, 24, 48, and 72 h post-transfection. The transfected cells (72 h post-transfection) were then treated with 5 and 10 $\mu\text{g/ml}$ S100A8/A9 for 48 h, and cell proliferation was assessed by MTT assays.

Blocking of RAGE with specific blocking antibody

Cells were grown in 96-well plates. After 72 h starvation in 1% ITS medium, they were treated with RAGE-blocking antibody (166 $\mu\text{g/ml}$) for 1 h and then treated with S100A8/A9 (5 and 10 $\mu\text{g/ml}$) for another 24 h. Proliferation was assessed using MTT assays.

Immunocytochemistry and confocal imaging

The 1% ITS starved cells were grown overnight on coverslips and then treated with 10 $\mu\text{g/ml}$ S100A8/A9. After 12 h, they were washed with PBS and fixed in 4% paraformaldehyde and then permeabilized with 0.1% Triton X-100. The cells were blocked with PBS containing 3% BSA (IgG- and protease-free). To locate RAGE or NF- κB -p50, the cells were incubated with anti-RAGE rabbit IgG (1:200 dilution) and anti-NF- κB -p50 goat IgG (1:100 dilution), respectively. After three washes with PBS, the RAGE and NF- κB -p50-antibody complexes were stained with the corresponding FITC (Sigma Co., 1:50 dilution) and Cy5-conjugated secondary antibodies (Sigma Co., 1:1,500 dilution) and then washed three times with PBS. The fluorescent images were then observed and analyzed using an Olympus-FV500 multilaser confocal microscope.

NF- κB activation in MCF-7 and MDA-MB231 cells after treatment with S100A8/A9

The ITS starved cells were cultured in six-well plates and treated with S100A8/A9 (10 $\mu\text{g/ml}$) for 8 h. The cells were scraped, and the nuclear fractions were prepared. NF- κB activation was analyzed using the Panomics Transbinding ELISA kit, according to the manufacturer's instructions.

Statistical analysis

The results were expressed as means \pm SD, and statistical differences were evaluated by one-way and two-way ANOVA followed by Tukey's post-hoc test using the software package SPSS 11 and Graphpad prism 4.0. $P < 0.05$ was considered significant.

RESULTS

S100A8/A9 at low micromolar concentrations promotes cell growth in different tumor cells

To investigate the putative cell growth-promoting activity of S100A8/A9, MCF-7, MDA-MB231, and SHEP cells were

starved in ITS-containing medium for 72 h, followed by treatment with increasing S100A8/A9 protein concentrations for different time intervals as indicated. Cell proliferation was determined by MTT assay (Fig. 1, A–C).

As obvious from Figure 1, S100A8/A9 exerts hypertrophic activity on MCF-7, MDA-MB231, and SHEP cell lines. S100A8/A9 at 10 $\mu\text{g/ml}$ induced significant cell growth ($P < 0.05$); however, the growth-promoting activity of S100A8/A9 reached a plateau or decreased at increasing protein concentrations and incubation periods of 36 h or 48 h (Fig. 1, A–C). Similar results were also obtained with Jurkat, BJAB, L929, HEK-293, and KELLY cells (data not shown). Next, the data were confirmed by using BrdU incorporation assay (Fig. 1, D and E). In agreement with the MTT assay, S100A8/A9 exerted cell growth-promoting activity. Higher S100A8/A9 protein concentrations did not increase cell proliferation if treatment was extended to 48 h.

S100A8/A9 specifically binds to MCF-7, MDA-MB231, and SHEP cells

Specific binding of S100A8/A9 to MCF-7 and MDA-MB231 cells was analyzed by a binding assay and evaluated by flow cytometry. The cells were incubated in the presence or absence of S100A8/A9, and the amount of bound protein was measured by flow cytometry using the FITC-labeled mAb 27E10, which specifically recognizes the S100A8/A9 heterodimer. The fluorescence in the absence of S100A8/A9 (nonspecific binding) was subtracted from the fluorescence determined in its presence. The data were analyzed using CellQuest Pro software.

As shown in Figure 2, A–C, MCF-7, MDA-MB231, and SHEP cells specifically bound S100A8/A9. The mean fluorescence intensities are shown in Figure 2D. Similar results were

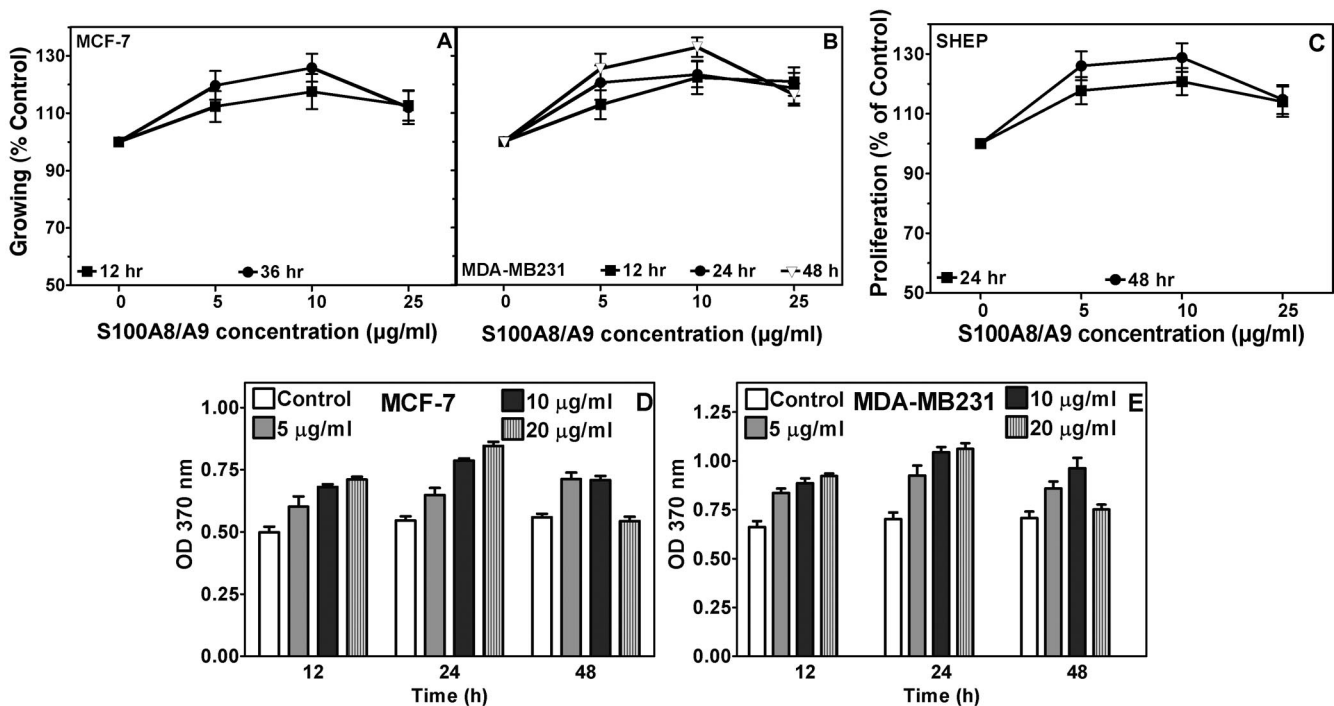


Fig. 1. Growth-promoting effect of S100A8/A9 on MCF-7 (A), MDA-MB231 (B), and SHEP (C) cells, which were treated with various concentrations of S100A8/A9 (0–25 $\mu\text{g/ml}$) for 12–48 h, and proliferation was assessed by MTT (A–C) and BrdU (D and E) assays. S100A8/A9 induced significant growth in all cell lines at all times ($P < 0.05$), and BrdU incorporation decreased significantly after 48 h ($P < 0.05$). Results are expressed as percentage of corresponding control and represent the mean \pm SD of four independent experiments.

also obtained with Jurkat, BJAB, HEK-293, L929, SHEP, and KELLY cells (data not shown).

RAGE is involved in cell growth signaling by S100A8/A9

As it has been suggested that RAGE serves as a primary extracellular membrane receptor of S100 proteins, RAGE expression was analyzed by Western blot. As shown in **Figure 3A**, a 50-kDa band was recognized by polyclonal anti-RAGE antibody. These data were confirmed by immunocytochemistry as shown in Figure 3, B and C.

To confirm that S100A8/A9 exerts its activity through RAGE, a protease protection assays was performed (Fig. 3D), similarly as it was described in a recent study, demonstrating that the extracellular region of RAGE (sRAGE) is protected from proteolytic digestion as a result of interaction with S100B [19]. When the tandem VC1 complex of RAGE was treated with chymotrypsin, full-length VC1 and the 25-kDa fragment were completely digested within 45–60 min in the absence of S100A8/A9 (left panel). In the presence of S100A8/A9, full-length VC1 and the 25-kDa fragment were clearly detectable after 60 min (right panel). These results provide direct evidence for a physical interaction between S100A8/A9 and the VC1 structural domain of RAGE.

To explore whether RAGE ligation was responsible for the cell growth-promoting activity of S100A8/A9, RAGE expression was inhibited in MDA-MB231 cells by RAGE-specific siRNA. Figure 3E shows that RAGE expression decreased with time as cells were treated with the specific RAGE-targeting siRNA. After 72 h, RAGE protein was nearly undetectable.

The specificity of the gene silencing was shown by the negative-control siRNA, which had no effect on RAGE expression. Then, S100A8/A9 binding was analyzed in MDA-MB231 cells treated for 72 h with RAGE-specific siRNA or negative-control siRNA by flow cytometry (Fig. 3F). Blocking of RAGE expression by the specific siRNA significantly reduced S100A8/A9 binding compared with untreated or negative-control, siRNA-treated cells, indicating that S100A8/A9 binds to RAGE.

We then investigated the cell growth-promoting activity of S100A8/A9 in MDA-MB231 cells that were treated with RAGE-specific siRNA or negative-control siRNA. As shown in **Figure 4A**, the cell growth-promoting activity of S100A8/A9 was significantly suppressed in cells where the expression of RAGE was also suppressed by the treatment with the RAGE-targeting siRNA ($P < 0.05$). Similar results were obtained with RAGE-blockage antibody in MDA-MB231 and SHEP cells, indicating that RAGE-mediated signaling is involved in the S100A8/A9-induced cell growth (Fig. 4, B and C).

S100A8/A9 induces sRAGE release from cells but does not induce HMGB1 release from the cells

sRAGE is produced in humans by alternative splicing of RAGE mRNA [26–28], and it has recently been shown that pericytes and endothelial cells produce and release sRAGE, suggesting the presence of a negative-feedback mechanism in RAGE signaling [26]. Therefore, we investigated the presence of sRAGE in the supernatant of S100A8/A9-treated cells to verify the possibility that S100A8/A9-induced release of sRAGE might act as a competitive receptor for cellular RAGE, thereby partly blocking the S100A8/A9-mediated cell growth. MDA-MB231 cells were treated with S100A8/A9 (15 $\mu\text{g/ml}$) for different time intervals (0–48 h) or increasing protein concentrations of S100A8/A9 (0, 10, 20, 25 $\mu\text{g/ml}$) for 36 h, and cell supernatants were subjected to Western blot using an antibody that recognizes both RAGE and sRAGE. As shown in Figure 4, D and E, S100A8/A9 treatment induced sRAGE release in cell culture media of MDA-MB231 cells in a time- and protein concentration-dependent manner. Similar data were also obtained for MCF-7 cells (data not shown).

Interestingly, S100A8/A9 treatment did not induce the release of HMGB1 from MDA-MB231 cells (Fig. 4F). These data were confirmed by a similar experiment using MCF-7 cells (data not shown). We observed a trace basic level of release of HMGB1 from MDA-MB231 and MCF-7 cells, which was not affected by S100A8/A9 treatment (Fig. 4F), and HMGB1 release was not observed in those cells treated with complete medium (data not shown). HMGB1 is a protein with key roles in maintenance of nuclear homeostasis. Surprisingly, a large body of experimental evidence demonstrates that HMGB1 is also endowed with extracellular signaling functions on various cell types using different receptors such as RAGE [29]. Thus, the protein has been included to the “alarmin” family, a term used by Oppenheim and co-workers [30] to identify a group of endogenous factors, also known as “endokines,” which once released in the extracellular space, interact with membrane receptors on immune cells to activate the inflammatory response [31]. Thus, theoretically, extracellular HMGB1 might provide a proliferation signal via RAGE. To test this possibility, MDA-MB231 cells were treated with S100A8/A9 (10 $\mu\text{g/ml}$) in the presence of anti-HMGB1 for 36 h, and cell

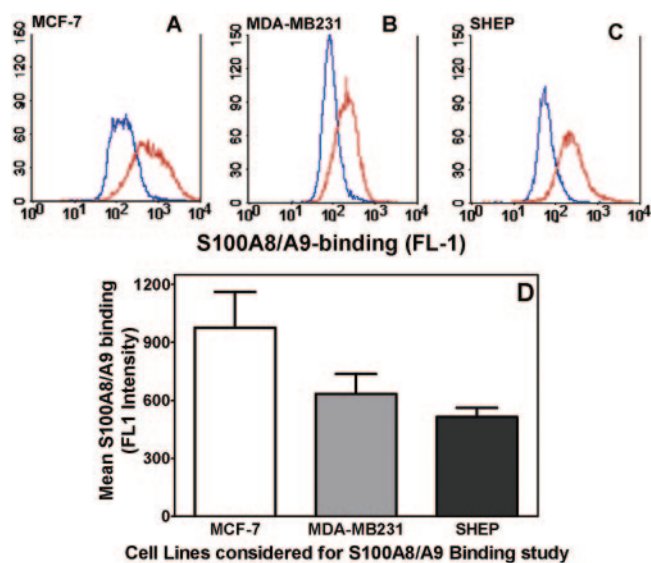


Fig. 2. Specific binding sites for S100A8/A9 on MCF-7 (A), MDA-MB231 (B), and SHEP (C) cells, which were incubated with 10 $\mu\text{g/ml}$ S100A8/A9 for 1 h on ice and washed three times with cold B-PBS. Then they were incubated with FITC-labeled, S100A8/A9-specific 27E10 antibody for 30 min on ice and finally washed three times with cold B-PBS. Cell-associated fluorescence [fluorescence 1 (FL-1)] was measured by flow cytometry. Blue histograms show nonspecific binding and red, total binding, respectively. (D) Mean fluorescence intensity (defined as mean fluorescence intensity of total binding–mean fluorescence intensity of nonspecific binding) of S100A8/A9.

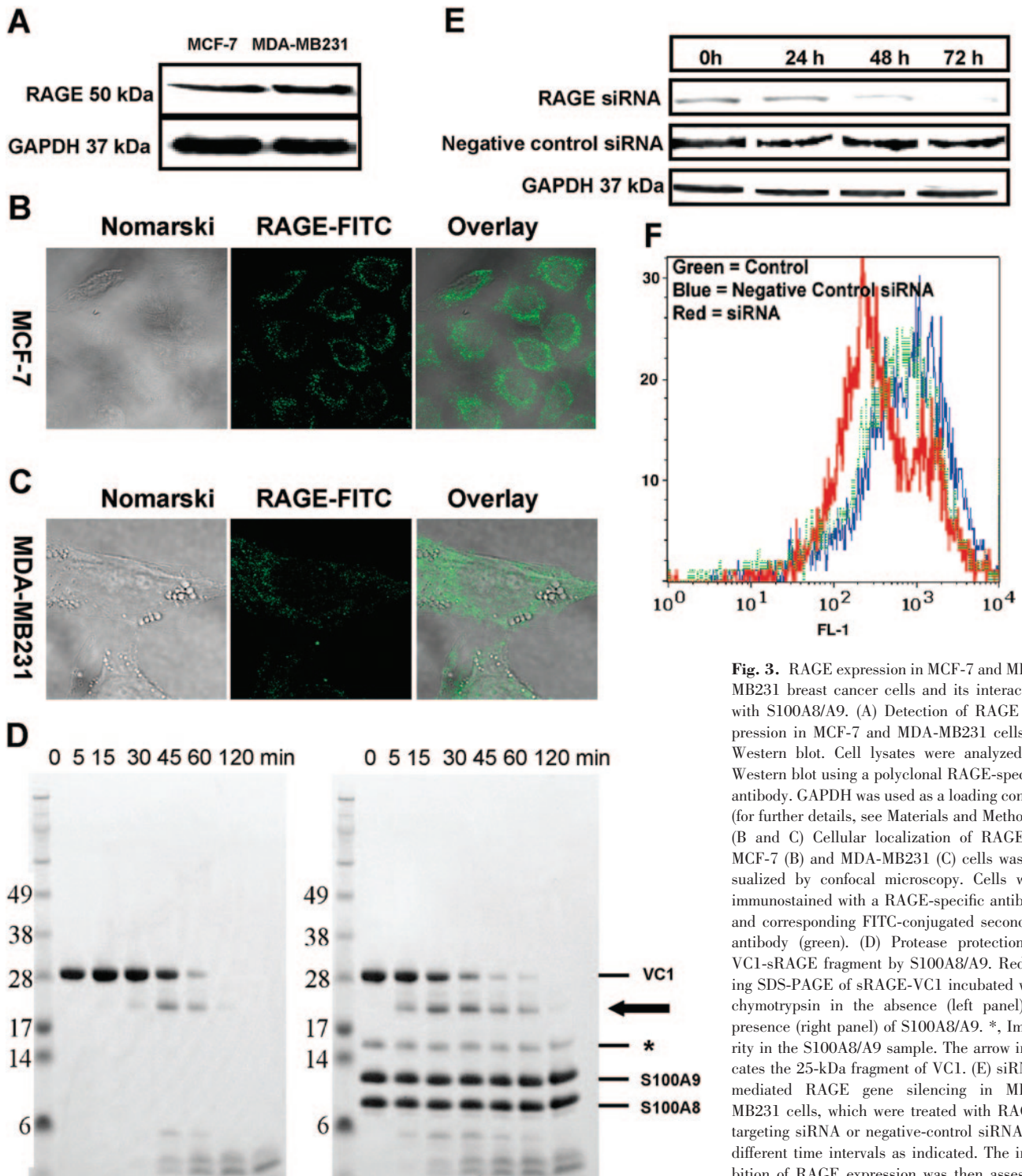


Fig. 3. RAGE expression in MCF-7 and MDA-MB231 breast cancer cells and its interaction with S100A8/A9. (A) Detection of RAGE expression in MCF-7 and MDA-MB231 cells by Western blot. Cell lysates were analyzed by Western blot using a polyclonal RAGE-specific antibody. GAPDH was used as a loading control (for further details, see Materials and Methods). (B and C) Cellular localization of RAGE in MCF-7 (B) and MDA-MB231 (C) cells was visualized by confocal microscopy. Cells were immunostained with a RAGE-specific antibody and corresponding FITC-conjugated secondary antibody (green). (D) Protease protection of VC1-sRAGE fragment by S100A8/A9. Reducing SDS-PAGE of sRAGE-VC1 incubated with chymotrypsin in the absence (left panel) or presence (right panel) of S100A8/A9. *, Impurity in the S100A8/A9 sample. The arrow indicates the 25-kDa fragment of VC1. (E) siRNA-mediated RAGE gene silencing in MDA-MB231 cells, which were treated with RAGE-targeting siRNA or negative-control siRNA for different time intervals as indicated. The inhibition of RAGE expression was then assessed by Western blot, using RAGE-specific anti-

body. GAPDH was used as a loading control. (F) Flow cytometric assessment of cell-surface binding of S100A8/A9 on MDA-MB231 in the absence (green) and presence of negative-control siRNA (blue) or RAGE-targeting siRNA (red). Cells were transfected with indicated siRNA, and after 72 h, the cells were stained with FITC-labeled, S100A8/A9-specific 27E10 antibody (see legend to Fig. 2 for further details).

proliferation was measured using MTT and BrdU assay. The results showed that anti-HMGB1 cotreatment did not significantly change the growth effect of S100A8/A9 ($P < 0.05$; data not shown).

Impact of S100A8/A9 on MAPK phosphorylation

RAGE ligation can activate multiple signaling pathways, including Ras-MAPK, PI-3K, protein kinase C, the JAKs, and transcrip-

tion factors, including STAT3, AP1, and NF- κ B [21, 32, 33]. However, the signaling mechanisms triggered by the ligation of RAGE in MCF-7 and MDA-MB231 cells remain unknown. Therefore, we first examined whether RAGE ligation by S100A8/A9 could activate p38, p44/42 MAPK, or SAPK/JNK. MDA-MB231 cells were treated with 10 μ g/ml S100A8/A9 for different time intervals, and cell lysates were analyzed by immu-

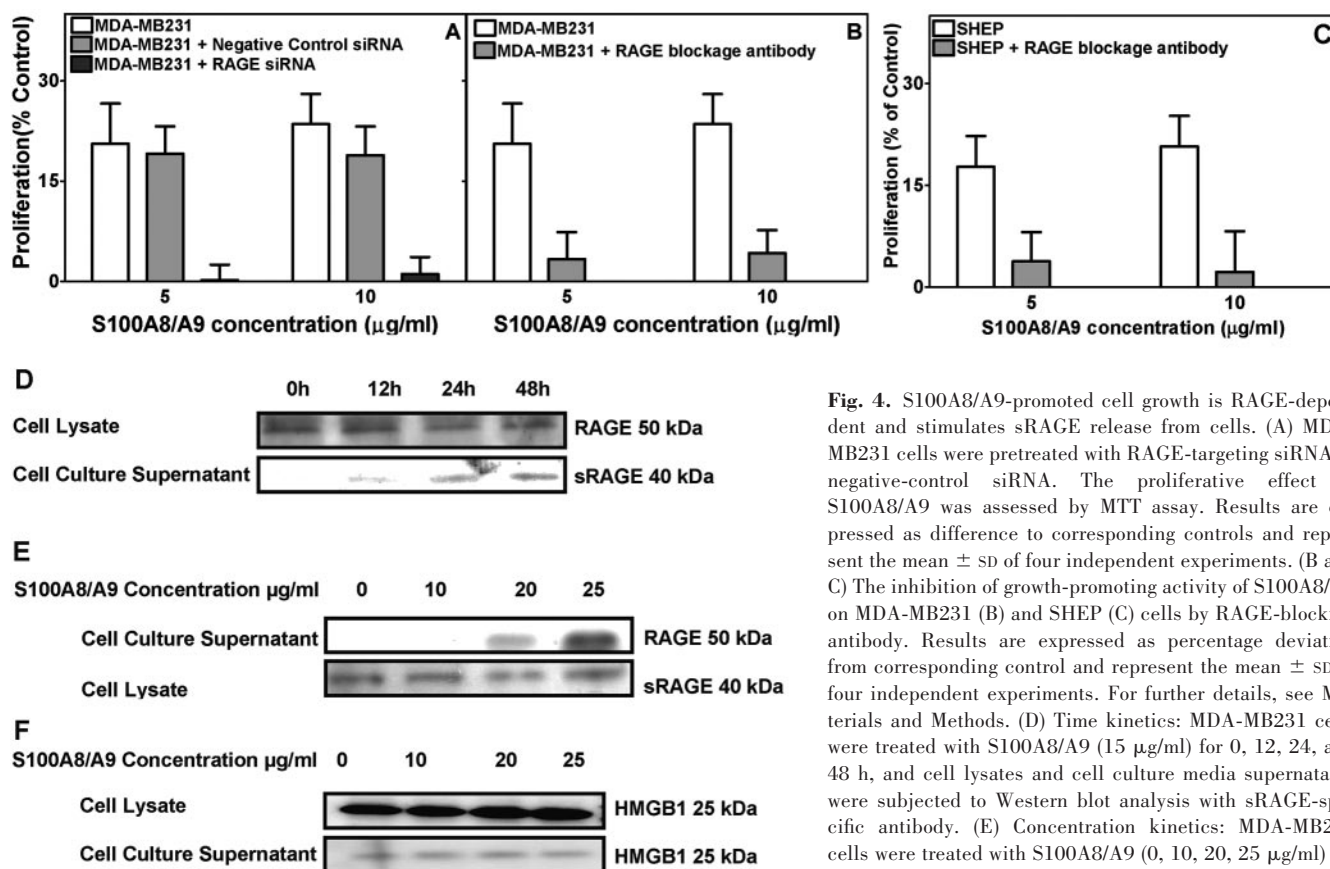


Fig. 4. S100A8/A9-promoted cell growth is RAGE-dependent and stimulates sRAGE release from cells. (A) MDA-MB231 cells were pretreated with RAGE-targeting siRNA or negative-control siRNA. The proliferative effect of S100A8/A9 was assessed by MTT assay. Results are expressed as difference to corresponding controls and represent the mean \pm SD of four independent experiments. (B and C) The inhibition of growth-promoting activity of S100A8/A9 on MDA-MB231 (B) and SHEP (C) cells by RAGE-blocking antibody. Results are expressed as percentage deviation from corresponding control and represent the mean \pm SD of four independent experiments. For further details, see Materials and Methods. (D) Time kinetics: MDA-MB231 cells were treated with S100A8/A9 (15 μ g/ml) for 0, 12, 24, and 48 h, and cell lysates and cell culture media supernatants were subjected to Western blot analysis with sRAGE-specific antibody. (E) Concentration kinetics: MDA-MB231 cells were treated with S100A8/A9 (0, 10, 20, 25 μ g/ml) for 36 h, and cell lysates and cell culture media supernatants were subjected to Western blot analysis with sRAGE-specific antibody. (F) MDA-MB231 cells were treated with S100A8/A9 (0, 10, 20, 25 μ g/ml) for 36 h, and cell lysates and cell culture media supernatants were subjected to Western blot analysis with HMGB1-specific antibody.

sific antibody. (F) MDA-MB231 cells were treated with S100A8/A9 (0, 10, 20, 25 μ g/ml) for 36 h, and cell lysates and cell culture media supernatants were subjected to Western blot analysis with HMGB1-specific antibody.

noblotting using suitable phosphospecific antibodies; GAPDH was included as loading control.

We analyzed by Western blot the amount of phosphorylated and nonphosphorylated kinases (Fig. 5A) along with densitometric, semiquantitative assessment of their phosphorylation (Fig. 5B). S100A8/A9 treatment rapidly induced phosphorylation of p38 (within 30 min) and p44/42 MAPKs (within 15 min), and phosphorylation was sustained up to 120 min. However, we failed to detect significant phosphorylation of SAPK/JNK. Similar results were obtained with MCF-7 cells (data not shown).

The above results implicate signaling through p38 and p44/42 MAPK pathways in S100A8/A9-induced cell growth. To verify their involvement, we performed proliferation assays in the presence and absence of specific kinase inhibitors. MCF-7 and MDA-MB231 cells were treated with S100A8/A9 (10 μ g/ml, 24 h) in the presence of the p38 MAPK inhibitor (SB203580, 10 μ M) and p44/42 MAPK inhibitor (U0126, 10 μ M). As shown in Figure 5, C and D, both inhibitors completely reversed the proliferation effect of S100A8/A9 on these cell lines.

NF- κ B activation was analyzed in MCF-7 and MDA-MB231 cells. After treatment with S100A8/A9 (10 μ g/ml) for 8 h, nuclear extracts were subjected to the NF- κ B-specific ELISA assay sensitive to the NF- κ B p50 subunit. Results showed an eightfold increase of NF- κ B activation in MDA-MB231 cells and a sixfold increase in MCF-7 cells, respectively (Fig. 6A). In contrast, pretreatment with RAGE-specific siRNA for 72 h abolished S100A8/A9-induced NF- κ B activation ($P < 0.0001$; Fig. 6B).

There was no significant difference in S100A8/A9-induced NF- κ B activation ($P > 0.05$) between control and those treated with negative-control siRNA (Fig. 6C). Finally, we explored the translocation of NF- κ B p50 in MDA-MB231 treated with S100A8/A9. As shown in Figure 6D, S100A8/A9 induced p50 translocation into the nucleus, and p50 remains in the cytosol in nonstimulated cells. These data indicate that S100A8/A9-promoted cell growth occurs through RAGE signaling and NF- κ B activation.

DISCUSSION

S100A8 and S100A9 appear to have a dual role in tumor biology. They help cells acquiring migratory activity by stimulating pseudopodia formation for invasion (invadopodia) [34] and exert growth-promoting activity as shown in the present study. On the other hand, we and others [15, 35–38] have demonstrated the proapoptotic effect of S100A8/A9 at higher protein concentrations. The apoptosis-inducing activity was within the range of 80–100 μ g/ml [15]. However, S100A8/A9 has cell growth-promoting properties at protein concentrations below 25 μ g/ml (Fig. 1). This finding is in agreement with a report of Huttunen et al. [18] demonstrating that nanomolar concentrations of another S100 family member, namely S100B, has growth-promoting effects in RAGE-expressing cells, whereas micromolar concentrations of S100B trigger apoptosis in an oxidant-dependent manner. S100B plays a role in brain trophism by acting as an intracellular regu-

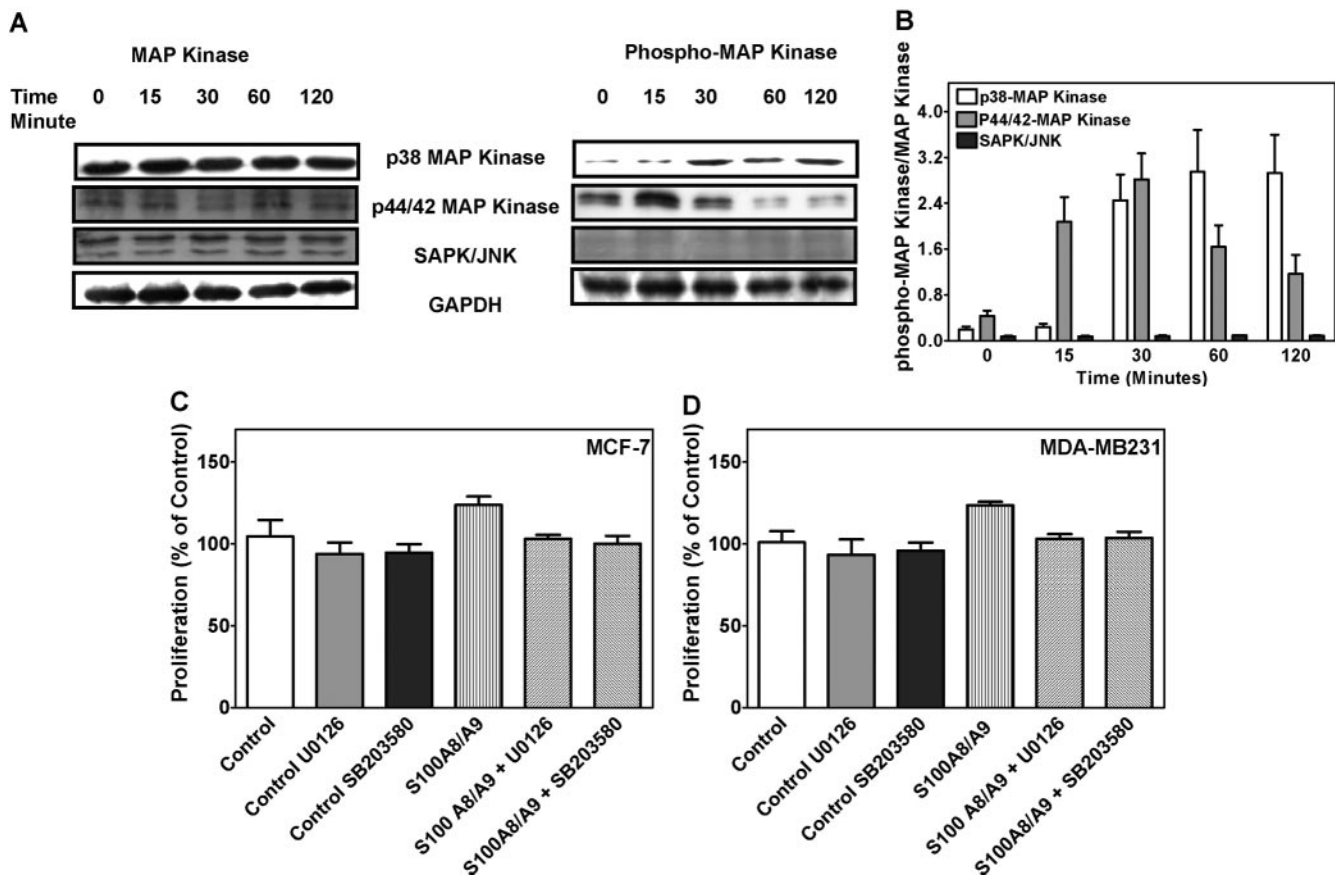


Fig. 5. S100A8/A9 treatment activates MAPKs but not SAPK/JNK. (A) MDA-MB231 cells were treated with S100A8/A9 (10 μ g/ml) for 0, 15, 30, 60, and 120 min, and cell lysates were analyzed by Western blot using the indicated antibodies. GAPDH was included as a loading control. (B) The quantities of phosphorylated and total kinases were estimated for triplicate of blotting by scanning of the Western blot membranes by "Storm" scanner and subsequent signal quantification by ImageQuant software. The intensity of experimental signals was compared with control and then normalized to GAPDH-loading control. (C and D) The S100A8/A9-proliferative effect was inhibited by SB203580 (p38 inhibitor, 10 μ M) and U0126 (p44/42 MAPK inhibitor, 10 μ M).

lator and an extracellular signal [33, 39]. Extracellular S100B regulates astrocytic, neuronal, and microglial activities, in part via engagement of RAGE [33, 39]. Interestingly, several cytokines exhibit a dual role: At low concentrations, they exert a trophic and protective effect, whereas at high concentrations, they cause cell death. Therefore, it could be concluded that S100A8/A9 has a dual function in cell death and survival similar to cytokines.

RAGE has been proposed to serve as a primary receptor for S100 proteins present in the extracellular space [17]. S100A12 and S100B are well established as ligands of RAGE [17], and the members of the S100/calgranulin family have common structural features and display sequence homology. However, the binding of S100A8/A9 to RAGE is still debated [40]. Therefore, we investigated whether RAGE ligation was responsible for the S100A8/A9-promoted cell growth. Among other experiments, we inhibited RAGE expression by pretreatment with RAGE-targeting siRNA. RAGE knock-down experiments provided strong evidence that RAGE is in fact the receptor for S100A8/A9, and RAGE-dependent signaling is involved in the cell growth-promoting activity of S100A8/A9 (Fig. 3). This finding was also confirmed by a RAGE-blocking antibody.

The interaction of RAGE with S100A8/A9 was further analyzed in a proteolysis protection assay using the VC1 fragment of RAGE (Fig. 3D). The extracellular region of RAGE consists

of one V-type Ig domain, followed by two C-type Ig domains. It has been shown recently that the V and C1 domains are not fully independent domains but rather, form an integrated structural unit [19]. In contrast, C2 is attached to VC1 by a flexible linker and is fully independent. Our data show that the presence of S100A8/A9 protects the VC1 fragment against chymotrypsin digestion, thereby confirming our initial hypothesis that S100A8/A9 binds and exerts activity through RAGE.

Furthermore, we could show for the first time that cells treated with S100A8/A9 release sRAGE (Fig. 4D). As it has been assumed that sRAGE competes with binding of ligands to RAGE, we conclude that this competition is responsible for the decrease in growth-promoting activity of S100A8/A9 at concentrations in the range of 25 μ g/ml. However, we note that RAGE does not seem to be the sole receptor for S100A8/A9. RAGE down-regulation by RAGE siRNA in MDA-MB231 cells did not completely inhibit the binding of S100A8/A9 to these cells (Fig. 3E). Therefore, we conclude that there is another, yet unknown, second receptor. A number of potential candidates for this activity have been reported in the last years, including heparan sulfate proteoglycan [40], carboxylated glycans [41], and fatty acid translocase/CD36 [42].

Activation of RAGE triggers several signal transduction pathways, including MAPK, Cdc42/Rac, JAKs, and NF- κ B signaling

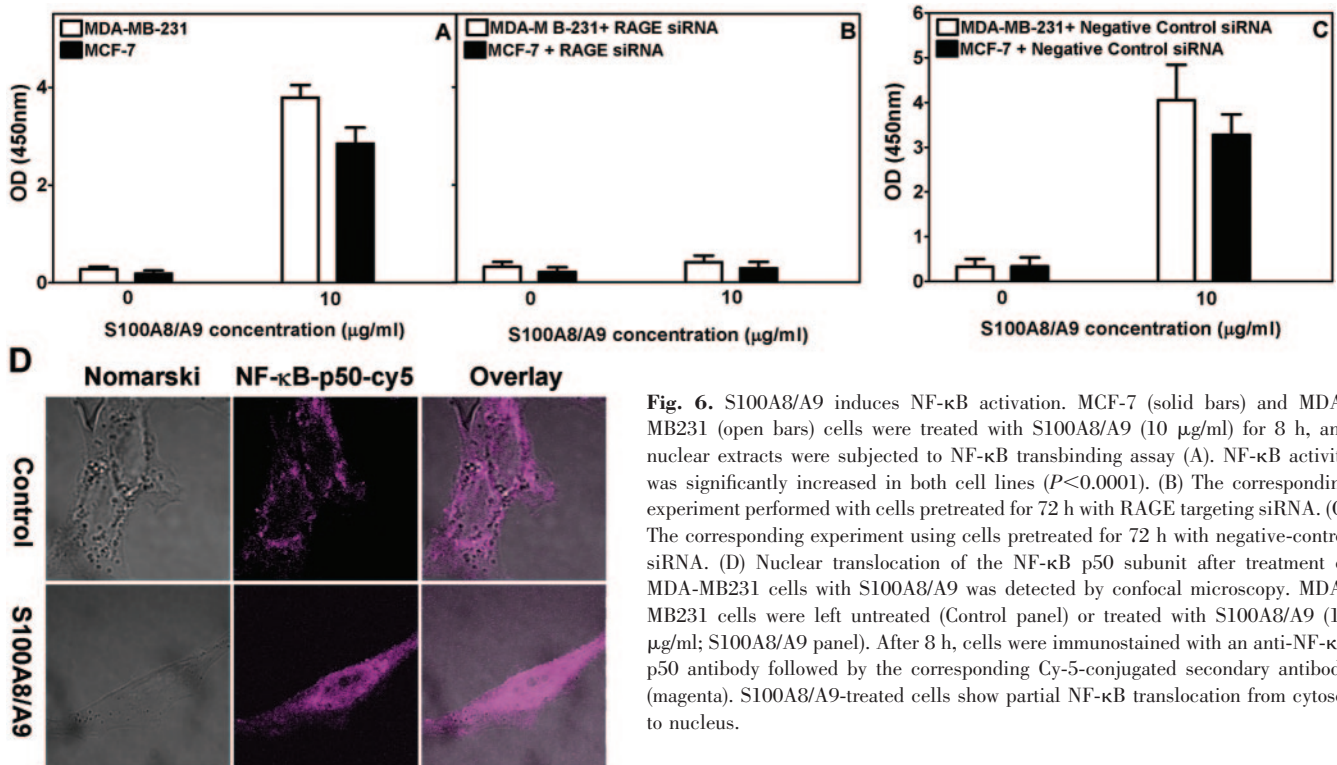


Fig. 6. S100A8/A9 induces NF-κB activation. MCF-7 (solid bars) and MDA-MB231 (open bars) cells were treated with S100A8/A9 (10 μg/ml) for 8 h, and nuclear extracts were subjected to NF-κB transbinding assay (A). NF-κB activity was significantly increased in both cell lines ($P < 0.0001$). (B) The corresponding experiment performed with cells pretreated for 72 h with RAGE targeting siRNA. (C) The corresponding experiment using cells pretreated for 72 h with negative-control siRNA. (D) Nuclear translocation of the NF-κB p50 subunit after treatment of MDA-MB231 cells with S100A8/A9 was detected by confocal microscopy. MDA-MB231 cells were left untreated (Control panel) or treated with S100A8/A9 (10 μg/ml; S100A8/A9 panel). After 8 h, cells were immunostained with an anti-NF-κB p50 antibody followed by the corresponding Cy-5-conjugated secondary antibody (magenta). S100A8/A9-treated cells show partial NF-κB translocation from cytosol to nucleus.

pathways, thereby influencing primary cellular events such as survival, motility, and the inflammatory response [21]. Consistent with other reports, we demonstrated that phosphorylation of p38 and p44/42 MAPK was induced after S100A8/A9 treatment (Fig. 5, A and B). These findings were confirmed by using specific p38 and p44/42 MAPK inhibitors (Fig. 5, C and D). However, we did not observe a significant phosphorylation for SAPK/JNK. Treatment with S100A8/A9 also caused NF-κB activation, as shown by a transbinding ELISA assay. This finding was confirmed by NF-κB p50 translocation studies and RAGE-blockage experiments and the fact that S100A8/A9-induced NF-κB activation could be blocked by inhibition of RAGE expression (Fig. 6).

In summary, we provide strong evidence that S100A8/A9 exerts cell growth-promoting activity at lower protein concentrations via RAGE-dependent signaling and subsequent phosphorylation of p38- and p44/42-MAPK as well as NF-κB activation. In contrast, RAGE knockdown did not reverse the apoptosis-inducing activity of S100A8/A9 at higher protein concentrations [34], indicating that the bimodal function of S100A8/A9 is mediated by two distinct receptors and signaling pathways.

Notably, primary tumors release soluble factors that induce the expression of members of the S100 protein family, primarily in lung and only minimally in liver or kidneys. The selective up-regulation of S100 proteins in lungs could facilitate the survival and proliferation of metastasizing cancer cells [43]. Thus, our findings might be useful for the development of strategies counteracting tumor metastasizing to certain organs. Our novel finding of cell growth-promoting activity of S100A8/A9 supports the concept that S100A8 and S100A9 play an important role in tumor growth and malignancy.

ACKNOWLEDGMENTS

S. G. and I. R. acknowledge fellowships from Manitoba Health Research Council (MHRC) and CancerCare Manitoba Foundation (CCMF). C. K. acknowledges support from Interdisciplinary Center for Clinical Research (IZKF; IZKF Project Ker3/086/04 to C. K.) and Deutsche Forschungsgemeinschaft (DFG; DFG Projects KE 820/4-1, KE 820/2-4, KE820/6-1, and KE 820/2-2). B. M. D. and W. J. C. acknowledge support from the U. S. National Institutes of Health (RO1 GM62112 and T32 GM08320). M. L. acknowledges support from Canadian Foundation for Innovation (CFI)-Canada Research Chair program and CCMF-, MHRC-, Canadian Institutes of Health Research (CIHR)-, and Manitoba Institute of Child Health (MICH)-funded programs. S. W. acknowledges support from the DFG We 1801/2-4 (S. W.), GRK1302 (S. W.), SFB 685 (S. W.), the German Federal Ministry of Education, Science, Research and Technology (Hep-Net; S. W.), the IZKF-Tübingen (Fö. 01KS9602; S. W.), the Wilhelm Sander-Stiftung (2004.099.1; S. W.), and the Landesforschungsschwerpunkt-programm of the Ministry of Science, Research and Arts of the Land Baden-Wuerttemberg. We thank Michael R. Miller for production of recombinant S100A8/S100A9.

REFERENCES

- Schafer, B. W., Heizmann, C. W. (1996) The S100 family of EF-hand calcium-binding proteins: functions and pathology. *Trends Biochem. Sci.* **21**, 134–140.
- Nacken, W., Roth, J., Sorg, C., Kerkhoff, C. (2003) S100A9/S100A8: myeloid representatives of the S100 protein family as prominent players in innate immunity. *Microsc. Res. Tech.* **60**, 569–580.

3. Hardas, B. D., Zhao, X., Zhang, J., Longqing, X., Stoll, S., Elder, J. T. (1996) Assignment of psoriasis to human chromosomal band 1q21: coordinate over-expression of clustered genes in psoriasis. *J. Invest. Dermatol.* **106**, 753–758.
4. Mischke, D., Korge, B. P., Marenholz, I., Volz, A., Ziegler, A. (1996) Genes encoding structural proteins of epidermal cornification and S100 calcium-binding proteins form a gene complex (“epidermal differentiation complex”) on human chromosome 1q21. *J. Invest. Dermatol.* **106**, 989–992.
5. Heizmann, C. W., Fritz, G., Schafer, B. W. (2002) S100 proteins: structure, functions and pathology. *Front. Biosci.* **7**, d1356–d1368.
6. Benedyk, M., Sopalla, C., Nacken, W., Bode, G., Melkonyan, H., Banfi, B., Kerkhoff, C. (2007) HaCaT keratinocytes overexpressing the S100 proteins S100A8 and S100A9 show increased NADPH oxidase and NF- κ B activities. *J. Invest. Dermatol.* **127**, 2001–2011.
7. Grote, J., Konig, S., Ackermann, D., Sopalla, C., Benedyk, M., Los, M., Kerkhoff, C. (2006) Identification of poly(ADP-ribose)polymerase-1 and Ku70/Ku80 as transcriptional regulators of S100A9 gene expression. *BMC Mol. Biol.* **7**, 48.
8. Arai, K., Yamada, T., Nozawa, R. (2000) Immunohistochemical investigation of migration inhibitory factor-related protein (MRP)-14 expression in hepatocellular carcinoma. *Med. Oncol.* **17**, 183–188.
9. Arai, K., Teratani, T., Nozawa, R., Yamada, T. (2001) Immunohistochemical investigation of S100A9 expression in pulmonary adenocarcinoma: S100A9 expression is associated with tumor differentiation. *Oncol. Rep.* **8**, 591–596.
10. Arai, K., Teratani, T., Kuruto-Niwa, R., Yamada, T., Nozawa, R. (2004) S100A9 expression in invasive ductal carcinoma of the breast: S100A9 expression in adenocarcinoma is closely associated with poor tumor differentiation. *Eur. J. Cancer* **40**, 1179–1187.
11. Ott, H. W., Lindner, H., Sarg, B., Mueller-Holzner, E., Abendstein, B., Bergant, A., Fessler, S., Schwaerzler, P., Zeimet, A., Marth, C., Illmensee, K. (2003) Calgranulins in cystic fluid and serum from patients with ovarian carcinomas. *Cancer Res.* **63**, 7507–7514.
12. El-Rifai, W., Moskaluk, C. A., Abdrabbo, M. K., Harper, J., Yoshida, C., Riggins, G. J., Frierson Jr., H. F., Powell, S. M. (2002) Gastric cancers overexpress S100A calcium-binding proteins. *Cancer Res.* **62**, 6823–6826.
13. Kong, J. P., Ding, F., Zhou, C. N., Wang, X. Q., Miao, X. P., Wu, M., Liu, Z. H. (2004) Loss of myeloid-related proteins 8 and myeloid-related proteins 14 expression in human esophageal squamous cell carcinoma correlates with poor differentiation. *World J. Gastroenterol.* **10**, 1093–1097.
14. Wang, J., Cai, Y., Xu, H., Zhao, J., Xu, X., Han, Y. L., Xu, Z. X., Chen, B. S., Hu, H., Wu, M., Wang, M. R. (2004) Expression of MRP14 gene is frequently down-regulated in Chinese human esophageal cancer. *Cell Res.* **14**, 46–53.
15. Ghavami, S., Kerkhoff, C., Los, M., Hashemi, M., Sorg, C., Karami-Tehrani, F. (2004) Mechanism of apoptosis induced by S100A8/A9 in colon cancer cell lines: the role of ROS and the effect of metal ions. *J. Leukoc. Biol.* **76**, 169–175.
16. Stulik, J., Osterreicher, J., Koupilova, K., Knizek, Macela, A., Bures, J., Jandik, P., Langr, F., Dedic, K., Jungblut, P. R. (1999) The analysis of S100A9 and S100A8 expression in matched sets of macroscopically normal colon mucosa and colorectal carcinoma: the S100A9 and S100A8 positive cells underlie and invade tumor mass. *Electrophoresis* **20**, 1047–1054.
17. Hofmann, M. A., Drury, S., Fu, C., Qu, W., Taguchi, A., Lu, Y., Avila, C., Kambham, N., Bierhaus, A., Nawroth, P., Neurath, M. F., Slattery, T., Beach, D., McClary, J., Nagashima, M., Morser, J., Stern, D., Schmidt, A. M. (1999) RAGE mediates a novel proinflammatory axis: a central cell surface receptor for S100/calgranulin polypeptides. *Cell* **97**, 889–901.
18. Huttunen, H. J., Kuja-Panula, J., Sorci, G., Agneletti, A. L., Donato, R., Rauvala, H. (2000) Coregulation of neurite outgrowth and cell survival by amphoterin and S100 proteins through receptor for advanced glycation end products (RAGE) activation. *J. Biol. Chem.* **275**, 40096–40105.
19. Dattilo, B. M., Fritz, G., Leclerc, E., Kooi, C. W., Heizmann, C. W., Chazin, W. J. (2007) The extracellular region of the receptor for advanced glycation end products is composed of two independent structural units. *Biochemistry* **46**, 6957–6970.
20. Kuniyasu, H., Oue, N., Wakikawa, A., Shigeishi, H., Matsutani, N., Kuraoka, K., Ito, R., Yokozaki, H., Yasui, W. (2002) Expression of receptors for advanced glycation end-products (RAGE) is closely associated with the invasive and metastatic activity of gastric cancer. *J. Pathol.* **196**, 163–170.
21. Taguchi, A., Blood, D. C., del Toro, G., Canet, A., Lee, D. C., Qu, W., Tanji, N., Lu, Y., Lalla, E., Fu, C., Hofmann, M. A., Kislinger, T., Ingram, M., Lu, A., Tanaka, H., Hori, O., Ogawa, S., Stern, D. M., Schmidt, A. M. (2000) Blockade of RAGE-amphoterin signaling suppresses tumor growth and metastases. *Nature* **405**, 354–360.
22. Arumugam, T., Simeone, D. M., Schmidt, A. M., Logsdon, C. D. (2004) S100P stimulates cell proliferation and survival via receptor for activated glycation end products (RAGE). *J. Biol. Chem.* **279**, 5059–5065.
23. Kerkhoff, C., Klempt, M., Kaefer, V., Sorg, C. (1999) The two calcium-binding proteins, S100A8 and S100A9, are involved in the metabolism of arachidonic acid in human neutrophils. *J. Biol. Chem.* **274**, 32672–32679.
24. Hunter, M. J., Chazin, W. J. (1998) High level expression and dimer characterization of the S100 EF-hand proteins, migration inhibitory factor-related proteins 8 and 14. *J. Biol. Chem.* **273**, 12427–12435.
25. Maddika, S., Bay, G. H., Krocak, T. J., Ande, S. R., Maddika, S., Wiehlec, E., Gibson, S. B., Los, M. (2007) Akt is transferred to the nucleus of cells treated with apoptin, and it participates in apoptin-induced cell death. *Cell Prolif.* **40**, 835–848.
26. Yonekura, H., Yamamoto, Y., Sakurai, S., Petrova, R. G., Abedin, M. J., Li, H., Yasui, K., Takeuchi, M., Makita, Z., Takasawa, S., Okamoto, H., Watanabe, T., Yamamoto, H. (2003) Novel splice variants of the receptor for advanced glycation end-products expressed in human vascular endothelial cells and pericytes, and their putative roles in diabetes-induced vascular injury. *Biochem. J.* **370**, 1097–1109.
27. Malherbe, P., Richards, J. G., Gaillard, H., Thompson, A., Diener, C., Schuler, A., Huber, G. (1999) cDNA cloning of a novel secreted isoform of the human receptor for advanced glycation end products and characterization of cells co-expressing cell-surface scavenger receptors and Swedish mutant amyloid precursor protein. *Brain Res. Mol. Brain Res.* **71**, 159–170.
28. Park, I. H., Yeon, S. I., Youn, J. H., Choi, J. E., Sasaki, N., Choi, I. H., Shin, J. S. (2004) Expression of a novel secreted splice variant of the receptor for advanced glycation end products (RAGE) in human brain astrocytes and peripheral blood mononuclear cells. *Mol. Immunol.* **40**, 1203–1211.
29. Dumitriu, I. E., Baruah, P., Manfredi, A. A., Bianchi, M. E., Rovere-Querini, P. (2005) HMGB1: guiding immunity from within. *Trends Immunol.* **26**, 381–387.
30. Yang, D., Chen, Q., Yang, H., Tracey, K. J., Bustin, M., Oppenheim, J. J. (2007) High mobility group box-1 protein induces the migration and activation of human dendritic cells and acts as an alarmin. *J. Leukoc. Biol.* **81**, 59–66.
31. Ulloa, L., Messmer, D. (2006) High-mobility group box 1 (HMGB1) protein: friend and foe. *Cytokine Growth Factor Rev.* **17**, 189–201.
32. Huttunen, H. J., Fages, C., Rauvala, H. (1999) Receptor for advanced glycation end products (RAGE)-mediated neurite outgrowth and activation of NF- κ B require the cytoplasmic domain of the receptor but different downstream signaling pathways. *J. Biol. Chem.* **274**, 19919–19924.
33. Donato, R. (2001) S100: a multigenic family of calcium-modulated proteins of the EF-hand type with intracellular and extracellular functional roles. *Int. J. Biochem. Cell Biol.* **33**, 637–668.
34. Hiratsuka, S., Watanabe, A., Aburatani, H., Maru, Y. (2006) Tumor-mediated upregulation of chemoattractants and recruitment of myeloid cells predetermines lung metastasis. *Nat. Cell Biol.* **8**, 1369–1375.
35. Nakatani, Y., Yamazaki, M., Chazin, W. J., Yui, S. (2005) Regulation of S100A8/A9 (calprotectin) binding to tumor cells by zinc ion and its implication for apoptosis-inducing activity. *Mediators Inflamm.* **2005**, 280–292.
36. Yui, S., Mikami, M., Tsurumaki, K., Yamazaki, M. (1997) Growth-inhibitory and apoptosis-inducing activities of calprotectin derived from inflammatory exudate cells on normal fibroblasts: regulation by metal ions. *J. Leukoc. Biol.* **61**, 50–57.
37. Yui, S., Mikami, M., Yamazaki, M. (1995) Induction of apoptotic cell death in mouse lymphoma and human leukemia cell lines by a calcium-binding protein complex, calprotectin, derived from inflammatory peritoneal exudate cells. *J. Leukoc. Biol.* **58**, 650–658.
38. Yui, S., Nakatani, Y., Hunter, M. J., Chazin, W. J., Yamazaki, M. (2002) Implication of extracellular zinc exclusion by recombinant human calprotectin (MRP8 and MRP14) from target cells in its apoptosis-inducing activity. *Mediators Inflamm.* **11**, 165–172.
39. Van Eldik, L. J., Wainwright, M. S. (2003) The Janus face of glial-derived S100B: beneficial and detrimental functions in the brain. *Restor. Neurol. Neurosci.* **21**, 97–108.
40. Robinson, M. J., Tessier, P., Poulson, R., Hogg, N. (2002) The S100 family heterodimer, MRP-8/14, binds with high affinity to heparin and heparan sulfate glycosaminoglycans on endothelial cells. *J. Biol. Chem.* **277**, 3658–3665.
41. Srikrishna, G., Panneerselvam, K., Westphal, V., Abraham, V., Varki, A., Freeze, H. H. (2001) Two proteins modulating transendothelial migration of leukocytes recognize novel carboxylated glycans on endothelial cells. *J. Immunol.* **166**, 4678–4688.
42. Kerkhoff, C., Sorg, C., Tandon, N. N., Nacken, W. (2001) Interaction of S100A8/S100A9-arachidonic acid complexes with the scavenger receptor CD36 may facilitate fatty acid uptake by endothelial cells. *Biochemistry* **40**, 241–248.
43. Ghavami, S., Kerkhoff, C., Chazin, W. J., Kadhoda, K., Xiao, W., Zuse, A., Hashemi, M., Eshraghi, M., Schulze-Osthoff, K., Klonisch, T., Los, M. (2008) S100A8/9 induces cell death via a novel, RAGE-independent pathway that involves selective release of Smac/DIABLO and Omi/HtrA2. *Biochim. Biophys. Acta* **1783**, 297–311.